

New Inclusion Assessment Method in Aluminum Alloys — Electrochemical Method for Inclusion Assessment (EcMIA)

XU Zhengbing, ZOU Yongzhi, ZENG Jianmin*

State Key Laboratory of Solidification Processing, Northwestern Polytechnical University, Xi'an 710072, China

Received June 8, 2010; revised November 29, 2010; accepted November **, 2010; published electronically November **, 2010

Abstract: The existence of inclusion influences the properties of aluminum alloy castings, from which the castings will face scrapping under severe condition. Great efforts on the inclusions in aluminum alloy was made and many inclusion assessment methods were put forward. However, most of the current methods are characterized by time consuming and expensive equipment cost, which limits the application in aluminum industry. Since the aluminum properties are sensitive to the inclusion, this paper tries to establish a new kind of inclusion assessment method. The inclusions were introduced to aluminum melts by adding aluminum scraps. The samples with different inclusion contents were prepared. The microstructure contained inclusions was observed. The inclusion was automatically identified with an image analyzer by setting different grey threshold value, and the inclusion content was obtained. The image analysis shows that inclusions wreck the continuity of the alloy matrix seriously, and the inclusion area percentage increases with the increasing of aluminum scraps. The high and low polarization measurements were conducted in 3.5 wt% NaCl aqueous solution at the temperature of 25 °C. The electrochemical parameters of the testing materials, such as corrosion potential E_k , corrosion current density I_k and the linear polarization resistance R_p , were obtained. The polarization measurement results show that the linear polarization resistances decrease, the corrosion potentials move towards more negative direction, and the corrosion current densities increase with the increasing of inclusion content. The theoretical analysis of the inclusion content and the corrosion current density was performed. The existence of inclusions makes the microstructure form corrosion microcells between the alloy matrix and inclusions. The impressed current can accelerate the current velocity or corrosion current density. The regression model of the inclusion contents vs. the corrosion current density was obtained. This model can be used to quantitatively analyze the inclusion content in aluminum alloys on the basis of inclusion sensitivity to the inclusion content. It is confirmed that the electrochemical method for inclusion assessment (EcMIA) is simple and reliable, which can provide a new solution for inclusion assessment in aluminum alloy.

Key words: aluminum alloys, inclusion assessment, electrochemical parameters, electrochemical method for inclusion assessment (EcMIA)

1 Introduction

Over the recent years, the trend towards aluminum alloys has been fuelled by a growing demand for stronger, lighter and corrosion resistant, especially in the aerospace and automotive industries^[1]. The current push for greater fuel efficiency, coupled with the control of the contents of hydrogen and inclusions^[1-3] and with the assessment of metal melts cleanliness.

Over the last 40 years, several techniques have been developed and used for assessing the cleanliness of molten aluminum casting alloys.

Porous disc filtration apparatus (PoDFA)^[4-6] developed

by Alcan Corp is a quantitative assessing method. But the representative of sampling still need further confirming, and new extraneous inclusions may be introduced into melt through the test. The PoDFA requires pressurized equipment, more important, micrograph, so the response time is rather long. Based on PoDFA, the Pressure filtration technique (Prefil Footprinter, by N-Tech Corp.) builds up a database of the relationship between inclusion content and filtration rate behavior. Sampling is the biggest problem like PoDFA, and the reproducibility is not better^[6, 7].

The samples are deformed to squeeze the inclusion into a small scope for observing inclusions more conveniently^[7]. The area of inclusions is measured quantitative by image analysis system. The method is easier than others of which both the morphology and the distribution of inclusions are reflected with its defined name of contaminant. In order to identify the inclusion content, the samples have to be machined and polished, so this is a time consuming method. Because of heterogeneous distribution of inclusions, the

* Corresponding author. E-mail: zjmg@gxu.edu.cn

This project is supported by National Natural Science Foundation of China (Grant No.50864002), Natural Science Foundation of Guangxi (Grant No.0991001), and Natural Science Foundation of Guangxi University of China (Grant No. X071081)

image analysis results show dispersion.

The liquid metal cleanliness analyzer (LiMCA) technique is based on the electrical resistive pulse principle^[8-10]. The electrical signal is used to calculate the particle density and size distribution by counting the number of pulses over period of measured time and by measuring their amplitudes. LiMCA, on the other hand, delivers an immediate response, but concerns small inclusions and seems best suited to measurement in continuous casting spouts. The result of inclusion measurement is expressed as a volume concentration in 10^6 scale, depending on the sampling tube. But the reliability of LiMCA need confirming further because of sampling in melts.

K-Mold is widely used fracture method for shop-floor evaluation in Japan^[11, 12]. The casting metal is poured into a notched bar chill mold and visually examining macro defects on the fracture surface in a series of bars. The K-factor is the number of defects seen per number of fracture surfaces examined.

The organic reagent bromine-boluene reacts with the metal matrix, and then inclusion is left only. So the inclusion content may be gained by weighing^[13, 14]. This is also a time consuming method. What's more, the method can not reflect the distribution and morphology of the inclusion.

The existence of inclusion affects the properties of alloys^[1]. So the property can reflect the inclusion content to some extent. In this paper, in order to obtain different contents of inclusion, aluminum scraps with six different weights were introduced in aluminum melts. The microstructure contained inclusions was observed through Leica DMRE microscope, and the inclusion content was obtained through Leica automatic image analyzer (LAIA). The effect of inclusion on electrochemical properties, corrosion potential E_k , linear polarization resistance R_p , and corrosion current density I_k of test materials was investigated. The effect of inclusion content on the corrosion current density I_k was analyzed theoretically in detail. The regression model between the corrosion current density I_k and inclusion content through image analysis^[4] was also established. On the basis of the above analysis, a novel inclusion assessment method electrochemical method for inclusion assessment (EcMIA) was presented in this work.

2 Experiments

2.1 Preparation of experimental materials

99.9% commercially pure aluminum with its machining scraps was used in this investigation.

Because of large specific surface area, the machining scraps are easy to produce oxides films. The oil contaminant and solid refractory particles are apt to be introduced into scraps and melts to form extraneous

inclusions.

The compositions of test materials are list as follows.

The materials were melt in high-frequency induction furnace (DUCATRON série 3). The melt was poured into sand molds without purification and with sample bar of 15 mm in diameter, and 100 mm in length. The samples were cut into 8 mm in thickness, and then were prepared for metallograph analysis and electrochemical test. All of specimens were wet ground to a 2 000 SiC, then polished to 0.5 μm diamond paste, and finally were washed with distilled water, ethanol and acetone.

Table 1. Compositions of the test samples (wt %)

| Samples No. | Pure aluminum | Aluminum scraps |
|-------------|---------------|-----------------|
| | w_a | w_{as} |
| 1# | 100 | 0 |
| 2# | 80 | 20 |
| 3# | 60 | 40 |
| 4# | 40 | 60 |
| 5# | 20 | 80 |
| 6# | 0 | 100 |

2.2 Principle of electrochemical experiment

2.2.1 Corrosion potential

Corrosion potential E_k , also called open circuit potential or free corrosion potential, is the potential when the corrosion of metal material reaches the equilibrium state without impressed current. It is an important parameter that characterizes the tendency of metal dissolving in salt solution^[15, 16-19].

The lower the corrosion potential is, the easier the metal material to be oxidized and dissolved in salt solution.

2.2.2 Polarization curves

The corrosion current density I_k can be converse to electrochemical velocity according to Faraday formula^[16, 17]. Therefore, the corrosion current density is usually used to characterize corrosion velocity.

The potential of corrosion metal electrode deviates from corrosion potential when the electrode is placed with impressed direct current. Denote by ΔE the deviation value of the corrosion metal electrode potential from corrosion potential, it is also called polarization value or overpotential.

The relationship between the polarization current density and overpotential is as follows^[16]:

$$I = I_k [\exp(\Delta E / \beta_a) - \exp(\Delta E / \beta_c)]. \quad (1)$$

This is the Butler-Volmer formula. Where, $\Delta E = E - E_k$, and E is the potential of the metal electrode, mV, and I is the polarization current density; β_a , β_c are the natural logarithm anodic and cathodic Tafel slope, respectively. When $|\Delta E| > \frac{4.605\beta_a\beta_c}{\beta_a + \beta_c}$, the electrode system reaches high

polarization.

In anodic high polarization, the cathodic reaction may be neglected, so the relationship between current density and overpotential can be expressed as

$$I_a = I_k \exp(\Delta E / \beta_a), \quad (2)$$

let $b_a = 2.303\beta_a$, then

$$E - E_k = b_a \lg(I_a / I_k), \quad (3)$$

the same for cathodic high polarization

$$E_k - E = b_c \lg(|I_c| / I_k), \quad (4)$$

where b_a , b_c are common logarithm anodic and cathodic Tafel slope, respectively; I_k is the corrosion current density; I_a , I_c are the anodic and cathodic impressed current density.

In high polarization state the overpotential has a linear relationship $\lg |I|$. The corresponding line slopes are the anodic and cathodic Tafel slopes b_a and b_c , respectively. As the two line are be extended to line of $\Delta E = 0$, that is $E_k = E$, I_k can be obtained.

2.2.3 Linear polarization resistance

When the overpotential is very low, $|\Delta E| \leq 10$ mV, the polarization is low polarization. In this condition, the second Taylor series extension of Eq. (1) is too small to be considered. Then^[16-20]

$$I = \frac{2.303(b_a + b_c)}{b_a b_c} I_k \Delta E, \quad (5)$$

or

$$I_k = \frac{I}{\Delta E} \square \frac{1}{2.303} \square \frac{b_a + b_c}{b_a b_c} = \frac{B}{R_p}. \quad (6)$$

It is can be seen that the overpotential ΔE is proportional to the impressed current density. The polarization curve is a line. The slope of the line is R_p ,

$R_p = \frac{\Delta E}{I}$, also called linear polarization resistance, with

dimensionality $\Omega \cdot \text{cm}^{-2}$; $B = \frac{1}{2.303} \times \frac{b_a + b_c}{b_a b_c}$. For a

certain corrosion system, B is constant.

The linear polarization resistance is an important thermodynamic parameter. It is believed that any obvious change of R_p can affect the corrosion velocity of corrosion system greatly.

2.3 Experiment procedure

The metallograph and inclusion analysis is carried out through Leica DMRE 1750 microscope.

The PS-168C is used to measure the electrochemical parameters. The test environmental temperature is $25 \pm 1^\circ\text{C}$, the corrosion medium is 3.5 wt% NaCl neutral solution, the tested metal materials is used as working electrode, the reference electrode is saturated calomel electrode (SCE), and the auxiliary electrode is platinum plate. The exposed area of samples was approximately 21 cm^2 .

The overpotential of low polarization is $|\Delta E| \leq 10$ mV (vs. E_k), and potential controlled scanning is employed with scanning rate 1 mV/s. The linear polarization resistance R_p is given by this measurement.

E_k is the equilibrium potential of the corrosion system without impressed current density (open-circuit). In high polarization, the overpotential ranges from $-1\ 500$ mV to $+1\ 500$ mV (vs. E_k), and the current controlled scanning with rate 1 mV/s is used. I_k is obtained from this test.

All of the polarization resistance (low polarization) and high polarization are measured 5 times respectively for every composition samples, and then all the data were statistically processed.

3 Results and Discussion

3.1 Metallograph analysis

This paper adopted the previous quantitative analysis method^[3], and 30 viewing fields were analyzed. The statistic quantitative information of inclusion area is listed in Table 2. Fig. 1 shows the optical images of materials.

Table 2. Results of image analysis of inclusions

| No. | Inclusion area percentage $\varphi/\%$ | Inclusion description |
|-----|--|---|
| 1# | 3.98 | Few, and porosity segregation |
| 2# | 4.70 | Inclusion segregation, porosity |
| 3# | 5.49 | Inclusion pieces, porosity increases |
| 4# | 6.92 | Larger inclusions and porosity |
| 5# | 8.14 | More inclusion segregated around porosity |
| 6# | 9.63 | Large number of inclusion blocks |

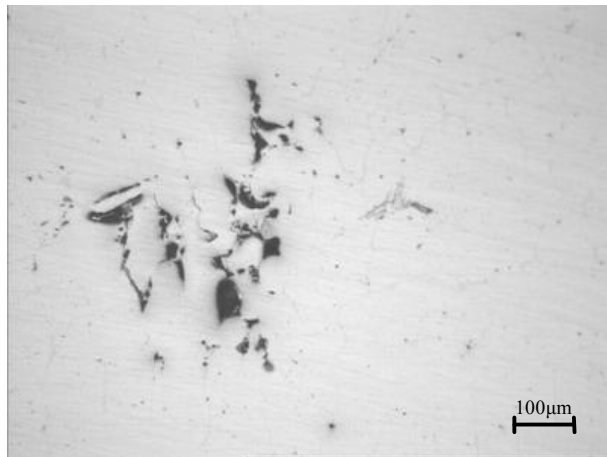
During trails, the melts surface was covered oxide films which protected the inner melt from further oxidizing. The time of melting is very short, so the reaction of the melts with water vapor or oxygen and the air entrainment can be neglected. It is believed the inner melts were clean. The morphology of commercial pure aluminum is shown in Fig. 1(a). Few inclusions and microporosity were found in pure aluminum morphology. The results of image analysis (see Table 2) also show that the inclusions area of sample 1# is the smallest, which agrees with the morphology photo.

The inclusion area increases with the amount of aluminum scraps increasing. The optical examination of microstructure found that most of microporosities appear in grain boundary, and the dark layered oxide films scatter in

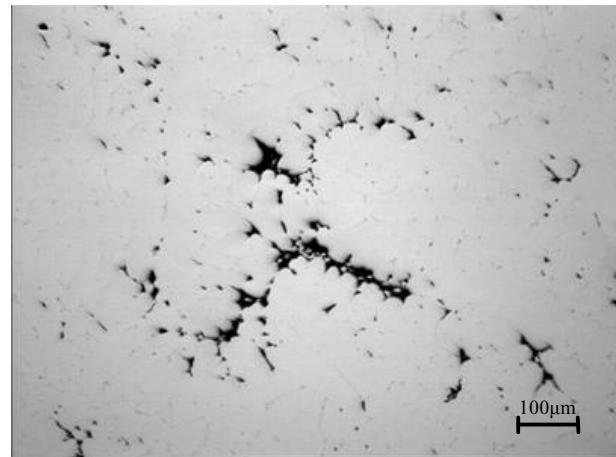
the material especially on the solidification front.

The image analysis and the statistic data processing show that inclusions in materials increase slightly at first, and then rapidly in sequence with the increasing of aluminum scraps. Because of large specific surface, the oxides films, solid particles, and oil contaminant are more dragged into melts by aluminum scraps to form inclusions

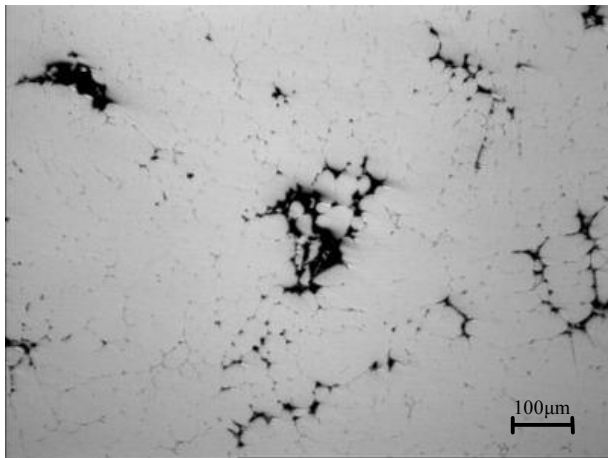
and to cause microporosity. When the solidification interface pushed forward, the extraneous inclusions above mentioned as the chief contributor blocked the feeding channel of melts. That resulted in the aggregation of inclusions, and contributed for the formation of dark-colored layer in microstructure (see Fig. 1(f)).



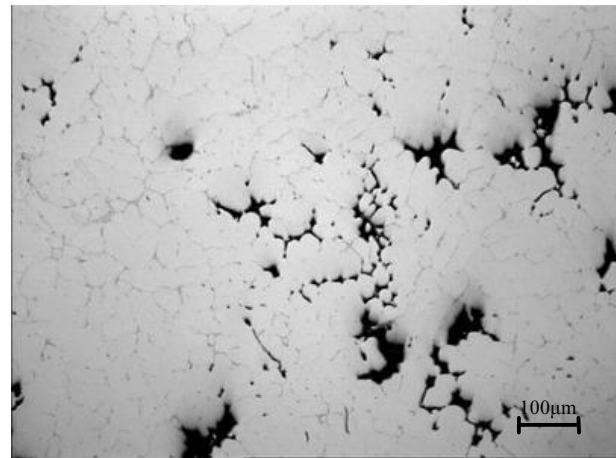
(a) 1#



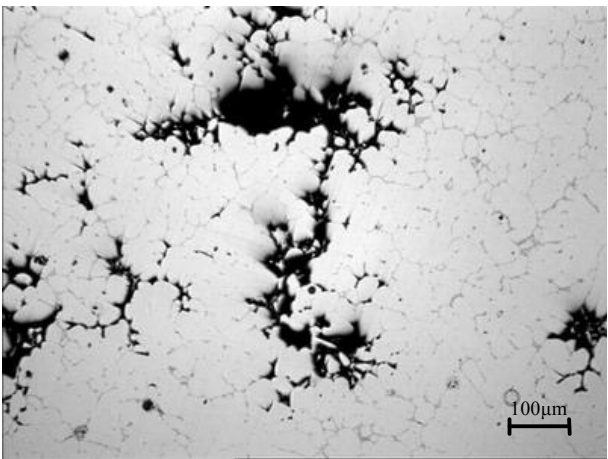
(b) 2#



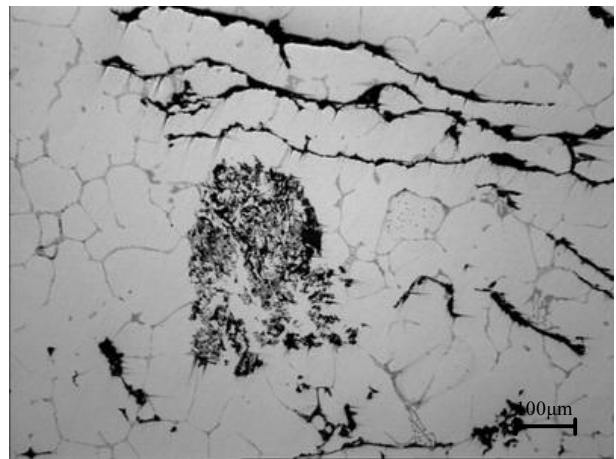
(c) 3#



(d) 4#



(e) 5#



(f) 6#

Fig. 1. Morphologies of inclusion of test samples with different aluminum scraps content

3.2 Electrochemical experiments analysis

3.2.1 Linear polarization resistance

Fig. 2 shows linear polarization resistance (R_p) of the test samples.

During low polarization, R_p is inversely proportional to corrosion current density, and is usually used as the parameter to monitor I_k . It is can be seen that once the aluminum matrix is mixed by any method, R_p rapidly decreases. Thus, the materials face more serious corrosion^[21].

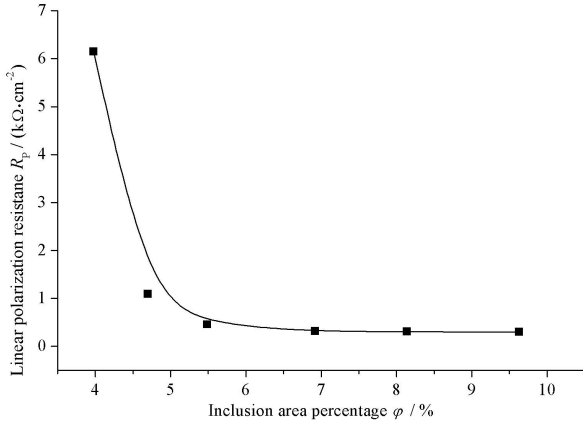


Fig. 2. Linear polarization resistance R_p

3.2.2 Polarization curves

Fig. 3 shows polarization curves of all of six groups of the test material. The corrosion potential and corrosion current density can be obtained through polarization curves fitting.

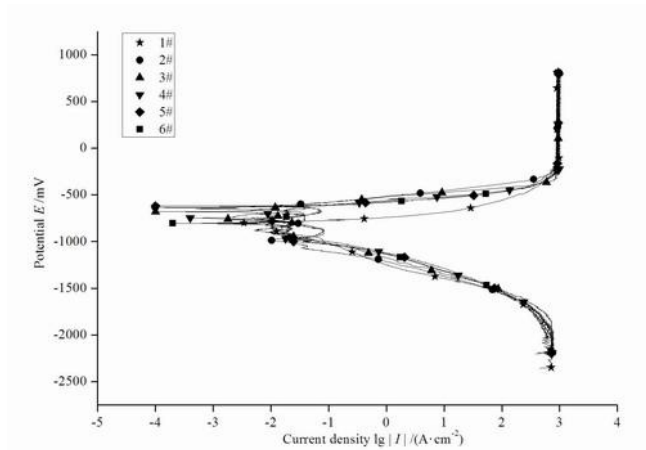


Fig. 3. Polarization curves of the test samples

3.2.3 Corrosion potential

The variation range of polarization overpotential included E_k . The half common logarithm diagram is usually used in polarization curves. The polarization process includes both low polarization and high polarization. The part of curves more than E_k is the anodic polarization, contrarily, the part of curves less than E_k is the cathodic polarization.

E_k is the equilibrium potential, and also is a significant

parameter for characterizing the corrosion tendency. Fig. 4 shows E_k of test samples.

Many factors affect metal working electrode reaction kinetic, such as the concentration of salt solution, temperature, pressure, and heat treatment, etc. The essential factor is the material itself, which is the purity of materials with the alloyed element.

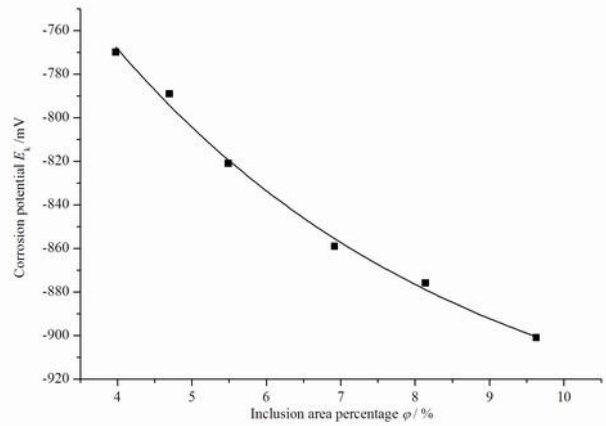
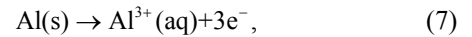


Fig. 4. Corrosion potential E_k of test samples

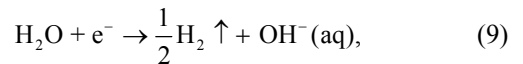
In essential, for this kind of corrosion system, the anodic reaction is the dissolution of Al:



the equilibrium potential of anode dissolution reaction is^[19]

$$E_{(\text{Al}/\text{Al}^{3+})} = \frac{\mu_{\text{Al}^{3+}} - \mu_{\text{Al}}}{3F}, \quad (8)$$

the cathodic reaction is the precipitation of H_2 :



the equilibrium potential of the reaction is

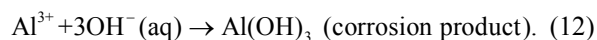
$$E_{(\text{H}^+/\text{H})} = \frac{\mu_{\text{H}} - \mu_{\text{H}^+}}{F}, \quad (10)$$

the energy condition of electrochemical corrosion is

$$E_k = E_{(\text{Al}/\text{Al}^{3+})} - E_{(\text{H}^+/\text{H})} < 0. \quad (11)$$

Firstly, aluminum dissolves and Al (aq) cations are produced (Eq. (8)), possibly through intermediate steps involving monovalent aluminum ion^[21]. Secondly, aluminum dissolution is accompanied by hydrogen

evolution (Eq. (10)), since aluminum in neutral and low pH aqueous solutions is well below the region of water stability. Finally, pH rises along with the cathodic reaction due to the formation of OH^- , which favors the formation of $\text{Al}(\text{OH})_3(\text{s})$ ^[21, 22]. Thus, the overall reaction could be expressed as



The metal material with more inclusions has smaller equilibrium potential. E_k decreases and moves to more negative direction. Thus, the metal material with inclusions is liable to corrosion.

3.2.4 Corrosion current density

Fig. 5 shows the corrosion current density (I_k) fitted from polarization curves.

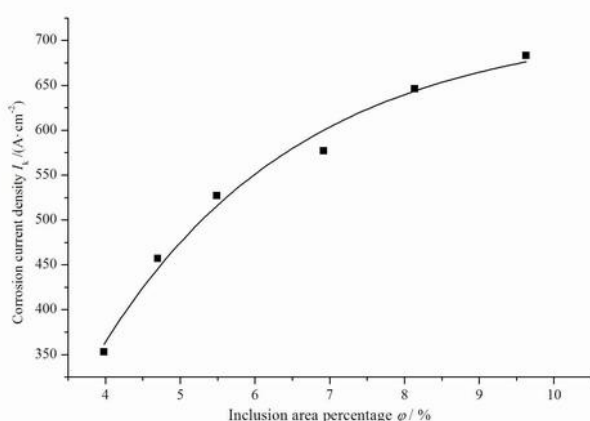


Fig. 5. Corrosion current density I_k of the test samples

In high polarization measurement, the kinetic parameter corrosion current density I_k can be obtained from the polarization curves^[23].

The results above show that I_k increases gradually with the increasing of inclusions.

Denoted by M the metal matrix, by I the inclusions. M and I can be considered as isolated electrodes when they contact. The corrosion potentials are E_{kM} and E_{kI} , and the corrosion current densities are I_{kM} and I_{kI} respectively. If $E_{kM} < E_{kI}$, M and I comprise corrosion microcell^[19]. When M and I are of short circuit, the common corrosion potential E_g is reached by polarization.

In this electrochemical corrosion system, it may be regarded that M and I form matrix/inclusions galvanic corrosion system. In the surface of M, the main reaction is the anodic dissolution reaction, the depolarizing agent reduction reaction may be neglected, and the matrix is a simple anode of corrosion cells. Correspondingly, in the surface of I, the main reaction is the cathodic depolarizing agent reduction, the reaction of anodic dissolution reaction may be neglected, and the inclusions are a simple cathode

of corrosion cells.

The corrosion system of two kind of contacted metals was studied elsewhere, and the relationship of corrosion current density with impurities area was given^[19].

For the system, in similar, let A_M the area of metal matrix, A_I the area of inclusions, and f the ratio of A_M/A_I , then the anodic dissolution corrosion current density is^[19]

$$\ln I_{aM} = \frac{E_{kI} - E_{kM}}{\beta_{aM} + \beta_{cI}} + \frac{\beta_{aM}}{\beta_{aM} + \beta_{cI}} \ln I_{kM} + \frac{\beta_{cI}}{\beta_{aM} + \beta_{cI}} \ln I_{kI} + \frac{\beta_{cI}}{\beta_{aM} + \beta_{cI}} \ln f, \quad (13)$$

If $A_M + A_I = A$, furthermore, A is constant. Under this condition, there has no extreme value at $\ln I_{aM}$ change curve with the A_I variation, because we have

$$\left(\frac{\partial I_{aM}}{\partial A_I} \right)_{A_M + A_I = A} = \frac{\beta_{aM}}{\beta_{aM} + \beta_{cI}} \times \frac{1}{(1-f)f} \times \frac{1}{A} > 0. \quad (14)$$

So $\ln I_{aM}$ always increases with the increasing of A_I or f .

From Eq. (13), it can be seen that the I_{aM} increases with the increasing of inclusions.

Fig. 5 illustrates the change of corrosion current density with the variation of inclusion content. The corrosion current density is the parameter that reflects the corrosion degree of materials. The larger the density is, and higher the corrosion velocity is, the faster the corrosion is. The results coincide well with the above theoretical analysis.

Eqs. (13) is simplified for theoretical discussion. In fact, the metal materials are always heterogeneous and all kinds of inclusions are distributed in metal matrix dispersedly. The inclusions are composed of other metallic or nonmetallic phases or particles. All of the electrochemical parameters of the inclusions are difficult to measure quantitatively. So it is necessary to find another way to characterize quantitatively the relationship between the corrosion current density and inclusion content. The empirical regression of I_k to the inclusion area is conducted in next section.

3.2.5 Regression Model

As mentioned above, the electrochemical properties changes obviously with the increasing of inclusion content. From another point of view, the changes of these properties can provide enough information of inclusion content. It is believed that this information can be used as an effective method to reflect quantitatively the inclusion content, which is called Electrochemical Method of Inclusion Assessment (EcMIA).

E_k reflects the reaction tendency of corrosion system, but it is not a corrosion kinetics parameter.

The metallograph analysis is the most basic method to study quantitatively inclusions. All of the methods of

inclusion assessment must be back to visual observation of inclusions except chemical analysis method. There is a close relationship between inclusions content and corrosion current density I_k . On the basis of the image analysis and electrochemical experiments, an empirical regression model EcMIA is developed to characterize the inclusion content in aluminum alloys:

$$\ln \varphi = 5 \times 10^{-6} I_k^2 + 0.025 I_k + 1.647 \quad (15)$$

The correlation coefficient of the regression equation 0.999 5 is obviously higher than the critical correlation coefficient 0.917 2 at the significance level 0.01. So it is believed that the regression is significant. The EcMIA was an efficiency method to assessment the inclusion content.

4 Conclusions

(1) The extraneous inclusions at the solidification interface blocked the feeding channel of melts, which resulted in the aggregation of inclusions, and contributed for the formation of dark-colored layer in microstructure. The results of image analysis show that the area of inclusions changes obviously with the increasing of scraps.

(2) The relationship between inclusion content and electrochemical parameters was revealed though electrochemical experiments. The corrosion potentials of test materials move to more negative direction, the polarization resistances decrease, and the corrosion current densities increase with the increasing of inclusions.

(3) The corrosion current density was sensitive to inclusion content change. The regression equation of between the corrosion current density and inclusion content was established:

$$\ln \varphi = 5 \times 10^{-6} I_k^2 + 0.025 I_k + 1.647 \quad 2$$

The regression coefficient (equals 0.999 5) shows high degree of statistic significant, which confirmed that the EcMIA can be used to evaluate the inclusion content of aluminum alloy.

References

- [1] SHU Da, SUN Baode, WANG Jun, et al. Melt purity-property relationships in casting aluminum alloys[J]. *Special Casting & Nonferrous Alloys*, 1992, 12(2): 52-56. (in Chinese)
- [2] ROOY E L. Hydrogen: The One-Third Solution[J]. *AFS Transactions*, 1993, 101: 961-964.
- [3] LI Huiling, YANG Yunlong, CUI Guoming, et al. The image analysis for degree of pinhole of aluminum alloy[J]. *Physical Testing and Chemical Analysis Part A: Physical Testing*, 2005, 41(12): 613-615. (in Chinese)
- [4] HABIBI Nasser. *Evaluation of inclusions and oxides in the aluminum-silicon alloys using Prefil technique*[D]. Chicoutimi: Universite du Quebec a Chicoutimi (Canada), 2002.
- [5] LIU L, SAMUEL F H. Assessment of melt cleanliness in A356.2

- aluminum casting alloy using the porous disc filtration apparatus technique Part I Inclusion measurements[J]. *Journal of Materials Science*, 1997, 32(22): 5 901-5 925.
- [6] LIU L, SAMUEL F H. Assessment of melt cleanliness in A356.2 aluminum casting alloy using the porous disc filtration apparatus technique Part II Inclusion analysis[J]. *Journal of Materials Science*, 1997, 32(22): 5 927-5 944.
- [7] CONG Rihong, BIAN Xiufang. Influence of the alloying element Cu on the hydrogen content in superheated aluminum melt[J]. *Special Casting & Nonferrous Alloys*, 2000, 20(3): 21-22. (in Chinese)
- [8] CAO Xin. A new indirect method of measuring the contents of solid inclusions in liquid aluminum alloys[J]. *Journal of Materials Science*, 2006, 41(13): 4 285-4 292.
- [9] TIAN C, LAW J, TOUW J van der, et al. Effect of melt cleanliness on the formation of porosity defects in automotive aluminum high pressure die casting[J]. *Journal of Materials Processing Technology*, 2002, 122(1): 82-93.
- [10] PEKGULERYUZ M O, PEDNEAU N. In-situ method for the investigation of equiaxed grain growth in hypoeutectic and hypereutectic Al-Si alloys[J]. *Scripta Materialia*, 1998, 38(10): 1 533-1 539.
- [11] LUO Feng, ZHAO Zhongxing, ZHAO Shuai. Research on detecting inclusion in aluminum liquid[J]. *China Foundry Machinery & Technology*, 2006(4): 11-13. (in Chinese)
- [12] LESSITER M J, RASMUSSEN W M. The dilemma of assessing your aluminum melt's cleanliness[J]. *Modern Casting*, 1996, 86(2): 45-48.
- [13] LU Shusun, GU Kaidao, ZHENG Laisu. *Nonferrous casting alloys & smelting*[M]. Beijing: National Defense Industry Publishing House, 1985. (in Chinese)
- [14] YANG Changhe, GAO Qin. *The purification of nonferrous alloys* [M]. Dalian: Dalian University of Technology Publishing House, 1989. (in Chinese)
- [15] LI Yitai, PANG Xingzhi, ZENG Jianmin. Study on high aluminum Zn-based alloys corrosion resistance[J]. *Special Casting & Nonferrous Alloys*, 2006, 26(7): 403-405. (in Chinese)
- [16] ZHAO Maiqun, LEI Ali. *Corrosion and protection of metal*[M]. Beijing: National Defense Industry Publishing House, 2002: 153-156. (in Chinese)
- [17] XIAO Jimei, CAO Chu'nan. *Principles of materials corrosion*[M]. Beijing: China Chemistry Press, 2002: 21-38. (in Chinese)
- [18] WANG Fengping, KANG Wangli, JING Hemin. *Fundamentals, methods and applications of corrosion electrochemistry*[M]. Beijing: China Chemistry Press, 2008: 166-208. (in Chinese)
- [19] CAO Chu'nan. *Principles of electrochemistry of corrosion*[M]. 3rd ed. Beijing: China Chemistry Press, 2008: 122-147. (in Chinese)
- [20] ZHAN Baohong, CONG Wenbo, YANG Ping. *Metallic electrochemical corrosion and protection*[M]. Beijing: China Chemistry Press, 2005: 25-45. (in Chinese)
- [21] PARDO A, MERINO M C, COY A E, et al. Corrosion behavior of magnesium/aluminum alloys in 3.5 wt.% NaCl[J]. *Corrosion Science*, 2008, 50(3): 823-834.
- [22] FELIV V, FELIV S. A noniterative method for determining corrosion parameters from a sequence of polarization data[J]. *Corrosion*, 1986, 42(3): 151-160.
- [23] MUYLDER J V, POURBAIX M. *Atlas of electrochemical equilibria in aqueous solution*[M]. Oxford: Pergamon Press, 1966: 139-145.

Biographical notes

XU Zhengbing, born in 1979, is a PhD candidate on material science and technology, State Key Laboratory of Solidification Processing, Northwestern Polytechnical University. He received his master degree on materials physical and chemistry, Guangxi University, China, in 2004. His research focuses on nonferrous

materials.

Tel: +86-771-3231238; E-mail: 51happiness@163.com

ZOU Yongzhi, born in 1978, is a PhD candidate on material science and technology, State Key Laboratory of Solidification Processing, Northwestern Polytechnical University, China. She received her master degree on materials physical and chemistry, Guangxi University, China, in 2004.

Tel: +86-771-3231238; E-mail: springzou@163.com

ZENG Jianmin, born in 1955, is a professor and a PhD supervisor in Guangxi University and Northwestern Polytechnical University. He received his PhD degree from State Key Laboratory of Solidification Processing, Northwestern Polytechnical University, China, in 1990. His research interests include nonferrous materials and processing, nonferrous casting, etc.

Tel: +86-771-3231238; E-mail: zjmg@gxu.edu.cn